

A Composite Photodetector with Wide Dynamic Range and Small Area for Dynamic Vision Sensor Application

Yaping Chen, Xiaona Zhu*, Shaofeng Yu*

School of Microelectronics, Fudan University, Shanghai 201203, China

*Corresponding Author's Email: {xiaona_zhu, shaofeng_yu}@fudan.edu.cn

ABSTRACT

In this paper, we design and simulate a photodetector with a photodiode-body-biased MOSFET (PD-MOSFET) and apply it to the dynamic vision camera (DVS). The parameters of the process and simulation are adjusted for the DC characteristics, spectral characteristics and transient response of PD-MOSFET. Compared with traditional photodiode (PD), the photocurrent of PD-MOSFET can be increased from $1.4e^{-12}A \sim 6.8e^{-7}A$. The spectral peak is around 550 nm and the latency range from 6 μ s (10^5lx) to 0.2s ($0.1lx$). DVS improves the dynamic range of PD-MOSFET to 120 dB compared to traditional DVS.

INTRODUCTION

Dynamic vision sensor (DVS) event camera is a new type of image sensor different from the traditional camera. It detects the change of light intensity through the photodiode (PD) of fixed area size. When the change of light intensity compared with the last event output exceeds the threshold, the polarity and position information generated by the event will be output. Because DVS uses logarithmic photoreceptors and the output reading of events are based on asynchronous address-event representation (AER) architecture, DVS can realize lower time latency and wider dynamic range, which means that the DVS can operate under high-speed scenes and challenging lighting conditions.

The development trend of DVS is to reduce the pixel area and improve the resolution [1]. As the pixel area is smaller and smaller, the photosensitive area of PD is smaller and smaller. The photocurrent is proportional to the photosensitive area of PD and decreases accordingly. Even the photocurrent is smaller than the leakage current of MOSFET in logarithmic photoreceptors, which leads to background noise increase and dynamic range decay. The dynamic range decayed to 90dB when the pixel size was reduced to 4.95 μ m [2].

This paper reports a photodiode-body-biased MOSFET (PD-MOSFET) that takes the p region of PD as the floating potential region adjusted by light intensity regulation, and then adjusts the substrate voltage of MOSFET next to PD, so that the light intensity can affect the drain current of MOSFET, and finally the drain current is input as the light current into the pixel processing circuit. In this paper, we adjust the process parameters by analyzing the DC, spectral and transient characteristics to verify that this device has great advantages in improving the dynamic

range of DVS with small pixel area.

DEVICE STRUCTURE

The detailed structure of PD-MOSFET is shown in Figure 1. The whole structure is realized in the N well of P substrate. Both the P substrate and the N well are grounded outside, which can isolate and control the substrate of MOSFET at a low potential. The optical window is above the photodiode with a size setting of 3 μ m \times 3 μ m, the polarity value of light is 0.5 and the wavelength is 550nm. The N^+ doping of the photodiode is $2e^{17}cm^3$ and the cathode external voltage is 1v. The source of the MOSFET is grounded, the drain terminal is connected to 0.3V, and the gate external voltage is -2.5V, so that the MOSFET works in the off-current region. Upon light exposure, electron-hole pairs are generated. Under the effect of the potential, part of the hole flows to the N well, part flows to the source terminal of MOSFET, while others accumulate to increase the potential in the P region and finally reach equilibrium. The change of the potential in the P region causes the output current of the MOSFET to change, which means the light intensity can change the output current of MOSFET.

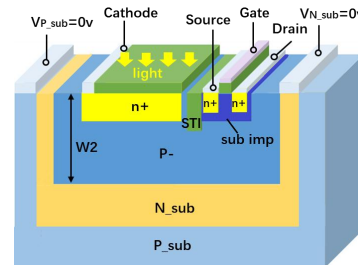


Fig.1. The structure of PD-MOSFET photodetector.

DC Characteristic

Figure 2 shows the relationship between the potential of the P region with light intensity under different doping concentrations in the P region. The potential in the P region is mainly determined by the longitudinal phototransistor structure in the photosensitive area, so the change of potential reflects the ratio of photogenerated current and triode leakage current. As the doping concentration in the P region changed from $1e^{12}cm^3$ to $1e^{16}cm^3$, the ability of PD-MOSFET to detect the lowest light intensity becomes higher and then lower, and finally the doping concentration in the P region is set to $1e^{15}cm^3$.

Figure 3 shows the relationship between the drain current of MOSFET and light intensity at different channel doping concentrations. The MOSFET in the off-current state is equivalent to a transistor, and adjusting the channel concentration is equivalent to adjusting the base region concentration. As the channel concentration changes from $1e^{16}cm^3$ to $1e^{17}cm^3$, the overall current of I_{ds} becomes lower, the range span becomes higher. Since the leakage current of the logarithmic photoreceptor is on the order of pA, the minimum current of I_{ds} should be greater than $1e^{12}A$, and the final channel doping concentration should be set to $7e^{16}cm^3$.

Figure 4 shows the relationship between the drain current of the MOSFET and the light intensity at different doping concentrations of source-drain terminal. The adjustment of the source-drain doping concentration is equivalent to the adjustment of the emission-collector region concentration in transistor. As the source-drain doping concentration increases from $1e^{18}cm^3$ to $1e^{19}cm^3$, the overall current of I_{ds} becomes higher and the range span becomes smaller. The photocurrent that the logarithmic photoreceptor can respond to normally is not greater than the order of uA, so the maximum current of I_{ds} should be less than $1e^{-6}A$. Since the source-drain doping concentrations should not be too low, and the adjustment of the source-drain doping concentration has little effect on the DC range of I_{ds} , this paper does not adjust the source-drain doping, but only changes the channel doping. The source-drain doping concentration is set to $1e^{19}cm^3$.

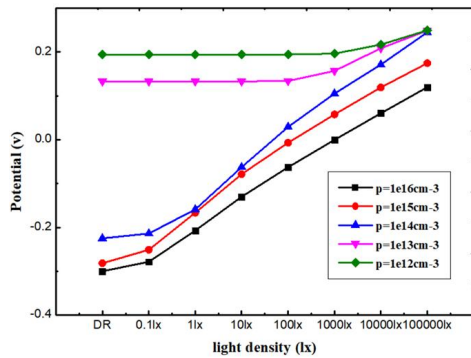


Fig. 2. The potential with light intensity at different doping concentrations of P region.

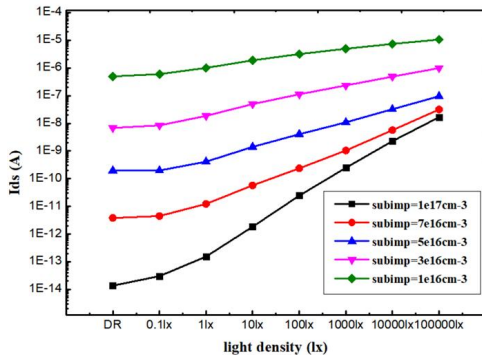


Fig. 3. I_{ds} with light intensity at different channel doping

concentrations.

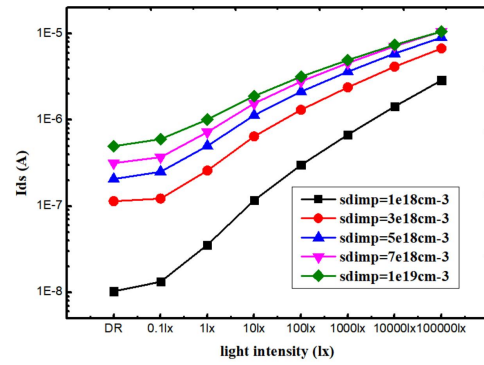


Fig. 4. I_{ds} with light intensity at different source-drain doping concentrations.

Spectrum Response

There are two main depletion regions of photosensitivity: one is the depletion region of the photodiode, and the other is the depletion region between the P region and the N well. Among them, the depletion region of the photodiode is inverse bias, and its position depends on the depth of N^+ doping; The depletion region between the P region and the N well is positively biased, and the position depends on the P region depth W_2 . The peak spectral response of the human eye is 550nm, and the photodetector should adjust the spectrum to match the spectral response of the human eye as much as possible.

Figure 5 shows the spectral response under different W_2 an illumination intensity of $0.0146mW/cm^2$. As the depth of W_2 ranges from $4\mu m$ to $2\mu m$, I_{ds} becomes slightly larger and the peak shifts left from 620nm to 550nm, and finally sets W_2 to $2.5\mu m$.

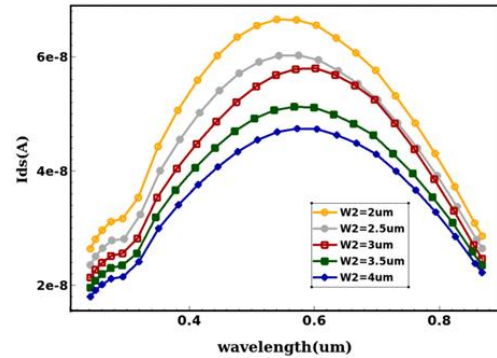


Fig. 5. I_{ds} with wavelegth at different depth of W_2

AC Characteristic and Circuit Implementation

DVS is mostly used for high-speed image capture, so the internal photodetector delay should be low to ensure high bandwidth [3]. The working process of this photodetector is divided into two steps: first, the photogenerated carrier charges the P region to raise the potential; Second, the MOSFET changes the output current

based on the change of substrate potential. Even though the PD-MOSFET can maintain a high gain in low light, it requires a low photocurrent to charge the capacitor. Therefore, the higher the light intensity, the smaller the delay of I_{ds} .

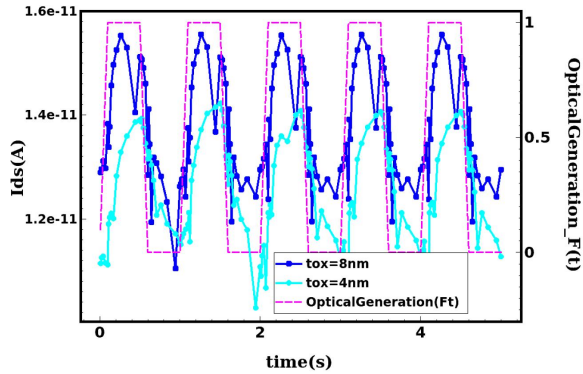


Fig. 6. Transient response at different tox.

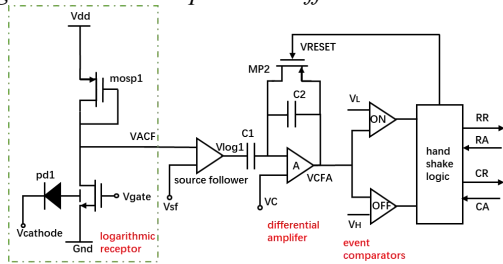


Fig. 7. Abstracted pixel schematic of DVS based on PD-MOSFET.

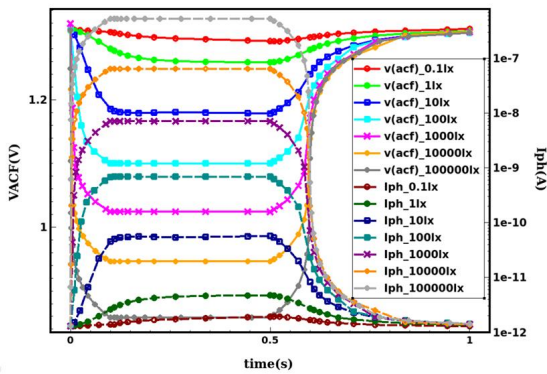


Fig. 8. Transient response of VACF and I_{ph} .

Cox is one of the important factors affecting the response latency. Figure 6 shows the instantaneous current response at a light intensity of $1.46e^{-8}W/cm^2$ and an oxide layer thickness of 4nm and 8nm. Upgrading from 4nm to 8nm makes I_{ds} larger, but the latency is shortened from 0.3s to 0.1s.

Figure 7 shows the internal circuit diagram of the DVS pixel [4]. The drain terminal of the PD-MOSFET is connected to the drain and gate terminals of mosp1. I_{ds} serves as the current source of mosp1, and VACF outputs the subthreshold voltage of mosp1. The Vdd was set to 1.8v.

Figure 8 shows the transient response of VACF and I_{ph} (I_{ds}) at different light intensity simulated by Mixmode, with the light intensity range increasing from 0.1lx to 10^5lx . As the light intensity increases, the VACF decreases and the delay of I_{ds} decreases.

Figure 9 shows that the VACF based on PD and PD-MOSFET changes with light intensity, which can be observed in the range of 0.1lx~ 10^5lx . The VACF after using PD-MOSFETs remains linear overall, and the dynamic range is extended to 120dB.

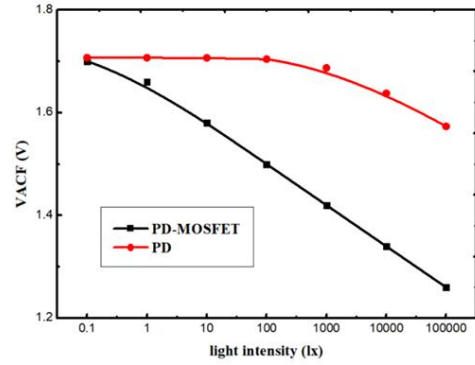


Fig. 9. VACF with light intensity of PD and PD-MOSFET.

CONCLUSION

This paper introduces a new type of PD-MOSFET hybrid structure photodetector. By adjusting the doping concentration in P region, channel doping concentration, P region depth W_2 , and gate oxide thickness, so that under the light intensity of 0.1lx~ 10^5lx , we make its photocurrent in the range of $1.4e^{-12}A$ ~ $6.8e^{-7}A$, the spectral peak is 550nm, and the response delay range is 0.1s~5us. DVS with PD-MOSFET extend the dynamic range to 120dB.

REFERENCES

- [1] Chi-Hang Chan, Lin Cheng, Wei Deng, et al. (2022). *Journal of Semiconductors*, 2022, vol.7.
- [2] Y. Suh et al., *2020 IEEE International Symposium on Circuits and Systems(ISCAS)*, 2020, pp.1-5.
- [3] M. Akrrai, N. Margotat, G. Sicard and L. Fesquet, *New Circuits and Systems Conference (NEWCAS)*, 2020, pp. 238-241.
- [4] P. Lichtsteiner, C. Posch and T. Delbruck, *Journal of Solid-State Circuits*, vol.43, Feb. 2008, pp.566-576.